PCA INVERSIONS FOR THE ROTATION OF THE SOLAR RADIATIVE INTERIOR

A. Eff-Darwich[1,2], S. G. Korzennik[3], S. Jimenez-Reyes[2], and R. A. García[4]

[1]*THEMIS S.L., C/ Vía Láctea s/n, Tenerife, 38205, Spain*
[2]*Instituto de Astrofísica de Canarias, C/ Vía Láctea s/n, Tenerife, 38205, Spain , Email:adarwich@themis.iac.es*
[3]*Harvard-Smithsonian Center for Astrophysics, Cambridge, MA, USA, Email:sylvain@cfa.harvard.edu*
[4]*Institute Service d'Astrophysique, CEA/DSM/DAPNIA, CE Saclay,91191, Gif sur Yvette, France, Email:rgarcia@cea.fr*

ABSTRACT

We present inferences of the rotation rate of the radiative interior, $0.18 < r/R_\odot < 0.66$, inverted from combined frequency splittings obtained for 2088-day-long time-series of GONG, MDI and GOLF observations. The frequency splittings were measured for modes with degrees between 1 and 25, and frequencies between 1.2 and 4.1 mHz. This corresponds to the largest frequency range used in an inversion of the rotational rate of the radiative interior. We also present a new inversion methodology based on Principal Component Analysis (PCA) as the smoothing factor used in a standard Regularized Least Squares (RLS) technique. Our inferences in the radiative interior reveal that the rotational rate is latitude independent and it decreases towards the core in the inner 35% of the solar interior.

Key words: Sun: Oscillations - Sun: Rotation.

1. INTRODUCTION

Helioseismic results confirm that the surface differential rotation persists throughout the convection zone (e.g. Schou *et al*, 1998; Thompson *et al*, 2003). There appears to be very little – if any – variation of the rotation rate with latitude in the outer radiative zone ($0.7 > r/R_\odot > 0.4$). In that region the rotation rate is almost constant (≈ 430 nHz), while at the base of the convection zone, a shear layer – the tachocline – separates the region displaying differential rotation throughout the convection zone from the one showing rigid rotation in the radiative zone.

Despite the large dispersion of the data sensitive to the deep interior ($0.2 < r/R_\odot < 0.4$), we can rule out an inward increase or decrease in the solar internal rotation rate down to $r/R_\odot \approx 0.3$, by more than 20% of the surface rate at mid-latitude (Chaplin et al., 1999; Eff-Darwich, Korzennik, & Jimenez-Reyes, 2002; Couvidat et al., 2003). This is in clear disagreement with the theoretical hydrodynamical models that predict a much faster rotation in the solar core (10 to 50 times faster than the surface rate).

More recently, García et al. (2004) and Korzennik (2004) developed new mode fitting procedures in an attempt to improve the quality of data sensitive to the rotation in the solar core. By using very long time series (in excess of 2000 days), they have measured rotational splittings for modes with frequencies as low as 1.2 mHz. We present here a first attempt to take advantage of these new data for which we have implemented a new inversion procedure to constrain the radial and latitudinal dependence of the rotation rate in the radiative interior with a particular emphasis on the solar core.

2. DATA SETS USED

The work presented here is based on rotational frequency splittings measured from observations by the GONG network and the MDI and GOLF experiments aboard SoHO. All rotational splittings data sets were obtained from 2088 days-long time series, starting 30 April 1996 and ending 17 January 2002. Table 1 summarizes the main characteristics of the data sets used in this work.

For all the data sets we subtracted the contribution to the frequency splittings of the rotation rate in the convective zone, namely

$$\begin{aligned}\Delta\nu_{n\ell m} &= \Delta_c\nu_{n\ell m} \\ &- \frac{1}{2\pi}\int_{r_t}^{R}\int_0^{\pi} K_{n\ell m}(r,\theta)\Omega(r,\theta)drd\theta \\ &+ \epsilon_{n\ell m} \qquad (1)\end{aligned}$$

where $\Delta_c\nu_{n\ell m}$ are the original frequency splittings and $\Delta\nu_{n\ell m}$ represent the frequency splittings after the subtraction of the convective zone contribution. The lower

Table 1. Description of the data sets used in this work, including name of the instrument, degree and frequency range of the data, and reference to the data analysis technique.

Instrument	Degree range	Frequency range (mHz)	Reference
MDI	4 - 25	1.1 - 3.9	Korzennik 2004
GONG	4 - 25	1.1 - 3.9	Korzennik 2004
MDI	1 - 10	1.7 - 3.9	Jiménez-Reyes et al. 2000
GOLF	1 - 2	1.1 - 2.0	García et al. 2004
GOLF	1	1.4 - 3.9	Gelly et al. 2002

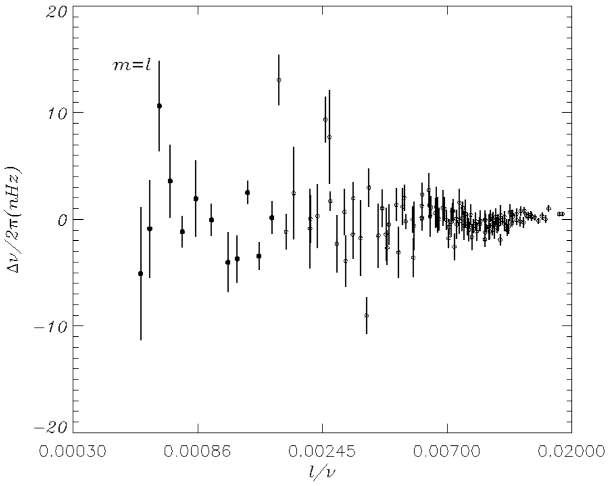

Figure 1. Sectoral frequency splittings used in the inversion procedure as a function of the internal turning point (≈ ℓ/ν). Filled circles represent the GOLF data by García et al. (2000), whereas open circles represent the MDI data derived by Korzennik (2004).

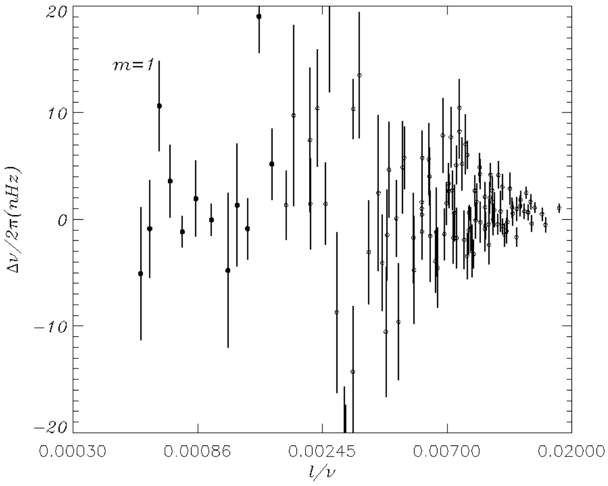

Figure 2. As in Fig. 1, but for modes with $m = 1$.

and upper bounds in the integral, r_t and R, represents the location of the tachocline and the solar surface, respectively.

Since our time series are very long (2088 days), very low frequency peaks are observed (down to $\nu \approx 1.2$ mHz) and hence high quality rotational splittings are added to the data sets used in the inversion procedures to infer the rotation rate of the solar interior.

For the work presented here, only the MDI and GOLF data obtained by Korzennik (2004) and García et al. (2004) were used in the inversion procedure. Figs. 1 and 2 show the frequency splittings for sectoral modes and modes with $m = 1$, respectively, as a function of the internal turning point. The two plots already indicate that both radial and latitudinal dependence of the rotation rate in the solar radiative interior is small.

3. PCA-BASED INVERSION METHODOLOGY

The principal component analysis (PCA) involves the transformation of a number of possibly correlated variables into a smaller number of uncorrelated variables called the principal components. The first principal component accounts for as much of the variability in the data as possible, and each succeeding component accounts for as much of the remaining variability as possible.

Let us define a series of physically reliable models for the rotation in the radiative interior. From these P models, we can calculate P artificial data sets, each one containing M rotational frequency splittings. In our case, M contains all frequency splittings for modes ranging from $\ell = 1$ to 25. We could calculate the correlation matrix for the artificial data sets and perform PCA on the correlation matrix. From the definition of PCA, the first p principal components will account for a good percentage of the variability in the data. In this sense, if the observational errors and noise of the data represents 1% of the total data value, we only need to keep the principal components that account for 99% of the data variability. From that perspective, PCA gives an intuitive way of understanding the resolving power of data in the solar radiative region.

The starting point of the PCA-based inversion methodology is the matrix relation that links the rotational frequency splittings and the rotation rate of the solar interior,

$$D = Ax + \epsilon \tag{2}$$

where D is the data vector, with elements $\Delta\nu_{n\ell m}$ and dimension M, x is the solution vector to be determined at N tabular points, A is the matrix with the kernels, of dimension $M \times N$ and ϵ is the vector containing the errors in D.

The RLS solution is the one that minimizes the quadratic difference $\chi^2 = |Ax - D|^2$, with a constraint given by a smoothing matrix, H, introduced in order to avoid the instabilities in the solution (Craig and Brown, 1986; Eff-Darwich and Perez-Hernandez, 1997). Hence, the estimated solution is given by

$$x_{est} = (A^T A + \gamma H)^{-1} A^T D \tag{3}$$

Let us define a set of P (in our case 550) template rotations, x_{art}, and the corresponding P template observables D_{art}. The correlation matrices for both sets of vectors are given by:

$$C_x = x_{art}^T x_{art} \tag{4}$$

and

$$C_D = D_{art}^T D_{art} \tag{5}$$

The rows of the matrices U_x and U_D obtained from the SVD analysis of the correlation matrices, are the principal components associated to the template rotations and observables, respectively.

The regularization process of the inversion methodology we are implementing is based on the fact that it is only necessary to retain o and p rows of the original matrices U_x and U_D to properly represent the template sets. Therefore, if the template sets are sufficiently general, any rotation distribution (and set of observables) that is not included in the rotation (and observables) templates could be represented by the first o and p principal components. In this sense, relation (2) may be re-written as

$$U_D^T D = U_D^T A U_x U_x^T x \tag{6}$$

where only the first o components of U_x and p components of U_D are retained. If we define $D' = U_D^T D$, $A' = U_D^T A U_x$ and $x' = U_x^T x$, relation 6 is transformed into

$$D' = A' x' \tag{7}$$

The unknown vector x' is then calculated following standard unconstrained matrix inversion

$$x' = (A'^T A')^{-1} A'^T D' \tag{8}$$

and finally the solution to the inversion problem is given by

$$x = U_x x' \tag{9}$$

A more detailed explanation of the inversion methodology will be soon available in Eff-Darwich et al. (2004)

4. RESULTS

In order to assess the reliability of the PCA-based inversion methodology, we present results for both, the actual inversion of the MDI+GOLF data set and the inversion of an artificial data set obtained from the following rotation profile:

$$\Omega(r,\theta) = \begin{cases} 442 & \text{for } r > 0.55R_\odot \\ & \text{and } \theta > 1.0 \\ 422 & \text{for } 0.35R_\odot > r > 0.55R_\odot \\ & \text{and } \theta > 1.0 \\ 422 & \text{for } r > 0.55R_\odot \\ & \text{and } 0.5 < \theta < 1.0 \\ 442 & \text{for } 0.35R_\odot > r > 0.55R_\odot \\ & \text{and } 0.5 < \theta < 1.0 \\ 437 & \text{for } r > 0.35R_\odot \\ & \text{and } \theta < 0.5 \\ 462 & \text{for } r < 0.35R_\odot \end{cases} \tag{10}$$

where θ is expressed in radians. From the length of the time series used to obtain frequency splittings, we could assure that the actual observational errors and data noise are well above 0.1 nHz. In this sense, we only have taken into account the principal components associated to the template observables that account for variabilities larger than 0.1 nHz. This leaves us with $p = 15$ principal components associated to the observables. The best solution in a χ^2 sense was obtained by setting the number of principal components associated to the template rotations to $o = 15$. For this case, the inversion results for both the actual and artificial data are shown in Figs. 3 and 4, respectively. Although we infer part of the latitudinal variations of the artificial rotation for $r > 0.35R_\odot$, the sensitivity to angular variations in the solar core is very limited. In the

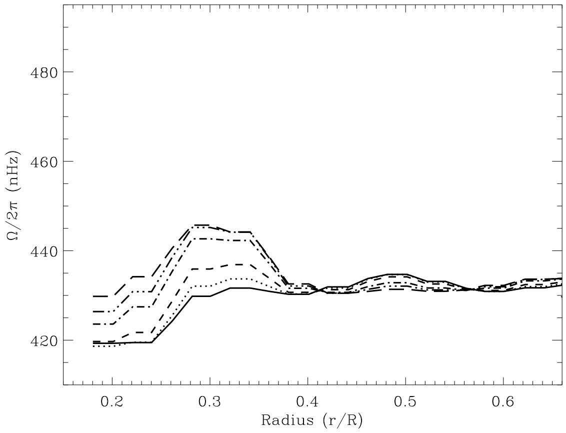

Figure 3. Inversion of the actual MDI+GOLF data set. Solid, dotted, dashed, dotted-dashed, triple-dotted-dashed and long-dashed represents the solution at the equator (π radians), 1.35, 1.10, 0.85, 0.60 and 0.35 radians, respectively.

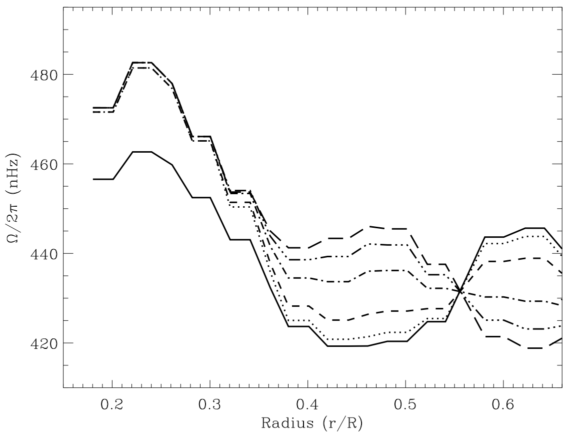

Figure 4. As in Fig. 3, but for the artificial data set

case of the inversion of actual observational data, we did not find significant latitudinal variations in the radiative zone, whereas a decrease in the rotation rate is observed at $r < 0.3R_{\odot}$.

We could find the exact solution to the inversion of the artificial data set when the number p of principal components account for variabilities as lower as 10^{-6} nHz, as shown in Fig. 5. This last inversion shows the power of the PCA-based methodology, however it is unrealistic, since it is not possible to get such precision in the observables. In summary, with an observational precision of ≈ 0.1 nHz, we have a fairly good radial resolution down to the solar core, but we have very limited latitudinal resolution for $r < 0.3R_{\odot}$.

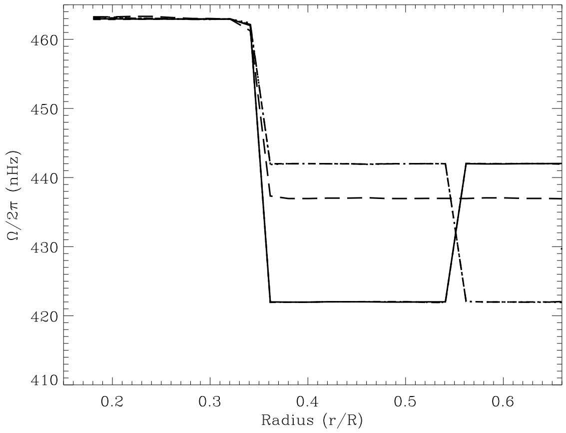

Figure 5. As in Fig. 3, but taking into account data variabilities as lower as 10^{-6} nHz.

REFERENCES

Chaplin, W.J., Christensen-Dalsgaard, J., Elsworth, Y., Howe, R., Isaak, G.R., Larsen, R.M., New, R., Schou, J., Thompson , M.J., & Tomczyk, S., 1999, MNRAS, 308, 405

Couvidat, S., García, R. A., Turck-Chièze, S., Corbard, T., Henney, C. J., & Jiménez-Reyes, S. 2003, ApJL, 597, L77

Craig, I. J. D. & Brown, J. C. 1986, Inverse problems in astronomy: A guide to inversion strategies for remotely sensed data, Research supported by SERC. Bristol, England and Boston, MA, Adam Hilger, Ltd., 1986, 159 p.,

Eff-Darwich, A., Pérez-Hernández, F., 1997, A&ASS, 125, 1

Eff-Darwich, A., Korzennik, S. G., & Jiménez-Reyes, S. J. 2002, ApJ, 573, 857

Eff-Darwich, A., Korzennik, S. G., , Jiménez-Reyes, S. J. Garcia, R.A., 2004, in preparation

Garcia, R. A., et al. 2004, Sol.Phys., 220, 269

Gelly, B., Lazrek, M., Grec, G., Ayad, A., Schmider, F. X., Renaud, C., Salabert, D., & Fossat, E. 2002, A&A, 394, 285

Jiménez-Reyes, S.J., 2000, Ph.D. thesis, Univ. La Laguna, Tenerife, (2000)

Korzennik, S.G., 2004, ApJ, submitted

Schou, J., *et al*, 1998, ApJ, 505, 390

Thompson, M. J., Christensen-Dalsgaard, J., Miesch, M. S., & Toomre, J. 2003, Ann. Rev. Astron. Astrophys., 41, 599